Research Article   **Open Access**

Effects of *Erwinia* sp. Infection on the Changes of Metabolisms in *Dendrobium officinale*

Xin Kong [1*], Jie Liu [1*], Jiyi Gong [1], Kamran Malik [2], Li Wang [1], Xianlei Chen [1], Ping Zhang [1], Jianfeng Wang [2,3]✉, Yin Yi [1]✉

1 Key Laboratory of National Forestry and Grassland Administration for Biodiversity Conservation in Karst Mountains Areas of Southwestern China, Key Laboratory of Plant Physiology and Developmental Regulation, School of Life Sciences, Guizhou Normal University, Guiyang, 550001, China

2 State Key Laboratory of Grassland Agro-ecosystems; Center for Grassland Microbiome; Collaborative Innovation Center for Western Ecological Safety; College of Pastoral Agriculture Science and Technology, Lanzhou University, Lanzhou, 730000, China

3 State Key Laboratory of Plateau Ecology and Agriculture, Qinghai University, Xining, 810016, China

✉ Corresponding author email: wangjf12@lzu.edu.cn; 100236417@qq.com

* These authors contributed equally to this work

Preferred citation for this article:

Kong X., Liu J., Gong J.Y., Malik K., Wang L., Chen X.L., Zhang P., Wang J.F., and Yi Y., 2022, Effects of *Erwinia* sp. infection on the changes of metabolisms in *Dendrobium officinale*, Molecular Plant Breeding, 13(16): 1-12 (doi: 10.5376/mpb.2022.13.0016)

Abstract The current study was aimed to investigate the changes in metabolites and metabolic pathways in *Dendrobium officinale* stem infected by *Erwinia* sp., the causal agent of *D. officinale*. A total of 176 metabolites were obtained by LC-MS in *D. officinale* before and after infection. Besides, the KEGG in MetaboAnalyst 5.0 (https://www.metaboanalyst.ca/) was used to analyze the pathways of the metabolites, of which only 73 metabolites were obtained Output ID from KEGG. The alanine, aspartate and glutamate metabolism, phenylalanine metabolism, isoquinoline alkaloid biosynthesis, lysine degradation, lysine biosynthesis, citrate cycle (TCA cycle), cutin, suberine, and wax biosynthesis, pyruvate metabolism, starch, and sucrose metabolism, and glyoxylate and dicarboxylate metabolism were the important metabolic pathways found by pathway enrichment analysis on KEGG ID. Furthermore, based on the information above, using VIP>1.0 and P<0.05 as screening criteria, there were only 68 differential metabolites among 73 metabolites. The metabolic pathways and differential metabolites analysis revealed that the contents of amino acid, organic acid, and nucleotides of EI (*D. officinale* infected with *Erwinia* sp.) plant were higher than EF (*D. officinale* free from *Erwinia* sp.) plant. Hence, *D. officinale* can enhance its structure by increasing the organic acids (citric acid, succinic acid, etc.) and amino acids (proline, arginine, etc.) to resist the pathogens.

Keywords *Dendrobium officinale*; *Erwinia* sp.; LC-MS; Metabolic pathways

Background

Dendrobium is an important genus of the Orchidaceae family and one of the largest genera, well-known for medicinal usage. About 1 000 species of *Dendrobium* are present globally while 74 species and 2 varieties are in China (Wang et al., 2011). *D. officinale* is the member of *Dendrobium*, which is a precious traditional Chinese herbal medicine and rich in polysaccharides, amino acids, alkaloids, and other substances, with high medicinal and edible value. *Dendrobium* can regulate the balance of Yin and Yang in the body, benefit the stomach and promote the production of body fluid (Liang et al., 2019). It has a use in making supplements and functional medicines (Yuan et al., 2020). However, due to over-exploitation and utilization of *Dendrobium*, its special habitat is highly fragmented and degraded. For instance, *D. officinale* is usually obtained from artificial herbs to meet the market demand. Artificial planting is often done in greenhouse cultivation and imitates the wild environment and under-forest planting methods (Zuo et al., 2020). However, some problems, such as high temperature, untimely replacement of substrates and improper management, etc., cause the occurrence of germs, pests, and diseases in dendrobium, resulting in the decrease of dendrobium yield and quality (Qiu et al., 2011). It is worth mentioning that *Erwinia* sp. is one of the most widely distributed pathogens that seriously affect the quality and yield of *D. officinale*.

The soft rot disease which severely damages the global crops is caused by the gram-negative bacterium *Erwinia* sp. (Feng, 2017). According to recent reports, soft rot pathogens exist in many cash crops, such as potato tubers (Zimnoch-Guzowska et al., 1999), bell pepper (Hua et al., 2019), taro (Wang et al., 2021), and *Dendrobium nobile*

(Balamurugan et al., 2020). Pathogens mainly enter into the plant through wounds, or natural openings if the conditions are suitable (Hua et al., 2019). After tissues are infected with pathogens, they compete with the host for nutrients to proliferate. At the same time, pathogens secrete a large number of extracellular enzymes, such as pectinase, cellulose, and pectinase to quickly dissolve the plant cell wall and to make the stems and fruits of plants rotten and soft.

Metabolomics approaches have developed rapidly in the last decade and played an important role in understanding plant resistance to biotic and abiotic stress. Thousands of metabolites, such as alkaloid (Razzaq et al., 2019), and flavonoids (Arbona and Gómez-Cadenas, 2015) have been synthesized in the process of plant evolution to adapt to nitrogen (Zhao et al., 2020), phosphorus (Sung et al., 2015) and other abiotic stresses. However, the complex chemical structure and dynamic behavior are the bottlenecks to determining the metabolites (Nikiforova et al., 2018). The development of modern technologies such as gas chromatography-mass spectrometry (GC-MS), liquid chromatography-mass spectrometry (LC-MS), and nuclear magnetic resonance spectroscopy (NMR) has enabled us to understand the adaptation mechanism of plants under adversity stress (Obata and Fernie, 2012; Razzaq et al., 2019). For example, infrared spectroscopy has been used to analyze the metabolomics of maize growth under different nitrogen nutrient conditions (Pavlík et al., 2010), the metabolite analysis of tomato leaves infected with *tomato yellow leaf curl virus* (TYLCV) using GC-MS technology (Sade et al., 2014), and the detection using LC-MS technology metabolites of 216 species of *Rhizoctonia solani* virus infected beans (Mayo-Prieto et al., 2019). These studies play an important role in understanding that crops are subjected to stresses, such as low nitrogen, insect pests, and other stresses.

Metabolomics helps to study the changing process of metabolites during the growth and development, and physiological changes during adversity stress to plants. However, little is known about the effects of *Erwinia* sp. on the changes of metabolisms in *D. officinale*. Therefore, metabolomics approaches were adopted to study the *Erwinia* sp. infection in *D. officinale.* The aim of this work was to investigate the effect of *Erwinia* sp. on the metabolic profile in *D. officinale*, to determine significantly different metabolites between EI and EF plants, and to determine important metabolic pathways of *D. officinale* in response to *Erwinia* sp.

1 Results

1.1 Metabolic changes

Our results revealed that 46 and 31 different metabolites were found in EI and EF plants under ESI+ and ESI-, respectively. According to the score plot of PCA, two groups of samples were significantly separated (*D. officinale* infected with *Erwinia* sp.: EI; *D. officinale* free from *Erwinia* sp.: EF). The results showed that (Figure 1a) the PCA scatter plot of *D. officinale* plant in ESI+, the PC1 and PC2 showed 51.8% and 11.9% of the total variance, respectively. The PCA scatter plots of *the D. officinale* plant in ESI- (Figure 1b) presented that PC1 and PC2 explained 43.7% and 13.3% of the total variance, respectively. The metabolomics data was analyzed by OPLS-DA to confirm the differences in the metabolic profiles of EI and EF plants in the positive ion mode. Q2 (cum) was used to estimate predictive power and R2Y (cum) was used to estimate the "goodness of fit" of the model (Jia et al., 2019). OPLS-DA was used to obtain pairwise comparison data. The score plot of OPLS-DA exhibited a significant difference between EI and EF plants under ESI+ conditions (R2Y=0.999; Q2=0.951) (Figure 1c). The significant difference between EI and EF plants in the ESI- condition (R2Y=0.998; Q2=0.928) indicated that the model was stable and reliable with a good predictive ability (Figure 1d). Significantly different metabolites were screened by VIP score (VIP>1) and t-test (P<0.05). The presence of *Erwinia* sp. may reprogram the metabolism pathway of the host.
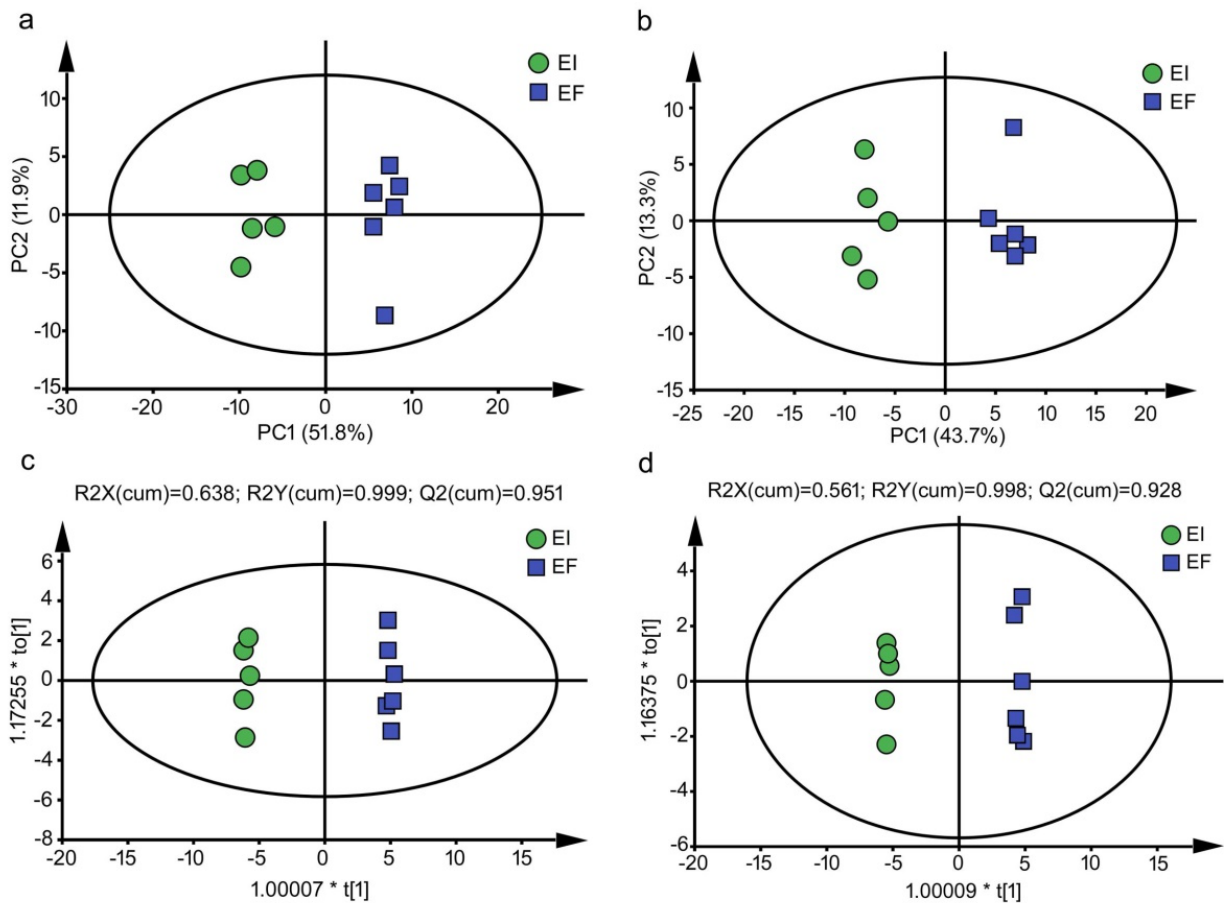
Figure 1 Plot of PCA scores

Note: metabolic plots of stems of EI and EF plants under ESI+ (a) and ESI- (b) conditions. OPLS-DA scores obtained under ESI+ (c) and ESI- (d) conditions show the effect of *Erwinia* sp. on the metabolism of *D. officinale* stems

1.2 Metabolic profiles of ESI+ and ESI- in response to *Erwinia* sp.

Under ESI+ condition, *Erwinia* sp. significantly altered 41 metabolites in *D. officinale* (Table 1). The presence of *Erwinia* sp. decreased the content of adenosine (0.51-fold), choline (0.48-fold), L-glutamine (0.59-fold), indole (0.81-fold), benzophenone (0.54-fold), cGMP (0.21-fold), 3,4-dihydroxyphenylglycol (0.12-fold), L-(+)-ergothioneine (0.17-fold), ricinoleic acid (0.15-fold), and phosphoglycolate (0.73-fold) compared to EF. But increased the content of L-histidine (5.97-fold), 2'-deoxyadenosine (3.44-fold), L-phenylalanine (11.14-fold), L-lysine (5.11-fold), betaine (4.45-fold), isoleucine (7.15-fold), D-(+)-tryptophan (6.89-fold), proline (3.70-fold), L-tyrosine 5.92-fold), asparagine (5.05-fold), hypoxanthine (34.70-fold), pipecolic acid (4.94-fold), 4-hydroxybenzaldehyde (6.30-fold), DL-arginine (5.07-fold), crotonic acid (9.69-fold), thymine (9.00-fold), cytosine (2.77-fold), acetophenone (3.99-fold), L-aspartic acid (4.06-fold), L-threonine (3.24-fold), L-(-)-methionine (10.94-fold), guanosine (3.38-fold), DL-2,6-diaminopimelic acid (5.48-fold), alpha-ketoglutaric acid (7.00-fold), D-pantothenic acid (2.47-fold), hexitol (7.07-fold), cytidine (1.96-fold), saccharopine (7.62-fold), pheophorbide A (183.54-fold), niacin (2.49-fold), stearidonic acid (2.64-fold), gamma-aminobutyric acid (9.81-fold), coumarone (4.94-fold), styrene (69.46-fold), uracil (2.37-fold), and toluene (4.83-fold). A total of 46 differentially expressed metabolites in *D. officinale* were influenced by *Erwinia* sp. in ESI+, with significant differences observed in the heat map (Figure 2a).

Table 1 Relative concentrations and fold changes of significantly different metabolites in EI and EF plants stem under ESI+

Metabolites name	EI	EF	$Log_2^{(EI/EF)}$
Adenosine	730.51±162.52	1438.06±278.43	-0.98
L-Histidine	661.07±126.39	110.71±21.05	2.58 **
2'-Deoxyadenosine	423.42±73.49	123.21±33.89	1.78 **
L-Phenylalanine	13019.62±3265.98	1168.78±116.31	3.48 **
L-Lysine	850.78±188.57	166.56±23.13	2.35 **
Betaine	7533.19±1219.47	1693.24±300.80	2.15 ***
Isoleucine	21114.48±3767.30	2953.39±879.55	2.84 ***
Choline	5361.61±1141.15	11158.00±1126.15	-1.06 **
D-(+)-Tryptophan	6223.61±1310.68	902.96±387.63	2.79 **
Proline	2428.19±356.87	657.13±81.36	1.89 ***
L-Glutamine	2392.61±440.33	4024.04±669.72	-0.75
L-Tyrosine	2401.42±591.53	405.33±138.55	2.57 **
Indole	2360.52±190.35	2897.70±176.51	-0.3
Asparagine	4375.68±779.49	866.02±386.17	2.34 **
Hypoxanthine	945.90±315.07	27.26±8.87	5.12 *
Pipecolic acid	976.91±216.02	197.82±26.80	2.30 **
4-Hydroxybenzaldehyde	196.47±43.42	31.20±12.27	2.65 **
DL-Arginine	2040.53±408.74	402.71±80.37	2.34 **
Crotonic acid	3095.89±582.09	319.40±35.71	3.28 ***
Thymine	140.79±32.20	15.64±0.85	3.17 **
Cytosine	353.93±21.50	127.72±18.72	1.47 ***
Acetophenone	659.92±280.67	165.51±47.73	2
L-Aspartic acid	935.76±109.15	230.64±32.11	2.02 ***
L-Threonine	1136.51±148.38	350.84±144.75	1.70 **
L-(-)-Methionine	881.81±149.31	80.62±29.58	3.45 ***
Guanosine	611.50±52.65	181.06±26.66	1.76 ***
DL-2,6-Diaminopimelic acid	211.28±33.93	38.54±4.47	2.45 ***
Benzophenone	105.61±17.51	195.94±20.85	-0.89 *
Alpha-ketoglutaric acid	250.05±56.43	35.74±5.70	2.81 **
D-Pantothenic acid	132.10±18.26	53.53±21.13	1.30 *
Hexitol	342.29±121.00	48.39±6.21	2.82 *
cGMP	27.35±22.38	128.97±35.40	-2.24 *
Cytidine	123.96±9.83	63.19±8.59	0.97 **
Saccharopine	51.00±23.47	6.69±0.52	2.93
3,4-Dihydroxyphenylglycol	20.67±10.69	168.32±18.42	-3.03 ***
Pheophorbide A	8822.71±1614.12	48.07±11.34	7.52 ***
Niacin	212.60±36.70	85.26±12.97	1.32 **
L-(+)-Ergothioneine	17.68±12.09	107.15±26.70	-2.60 *
Ricinoleic acid	15.33±5.44	99.90±26.76	-2.70 *
Stearidonic acid	885.53±211.95	335.57±71.39	1.40 *
Gamma-aminobutyric acid	3377.60±634.00	344.27±36.35	3.29 ***
Coumarone	755.33±147.17	152.95±45.24	2.30 **
Phosphoglycolate	6551.08±529.20	8982.96±768.29	-0.46 *
Styrene	1144.36±485.47	16.48±4.58	6.12 *
Uracil	152.46±17.02	64.22±7.85	1.25 ***
Toluene	107.78±29.28	22.33±1.65	2.27 *

Note: Fold changes were calculated using the formula $log_2^{(EI/EF)}$. *, **; *** means significant differences at $0.01<p<0.05$; $0.001<p<0.01$ and $p<0.001$, respectively

Under the condition of ESI-, 31 metabolites were significantly altered in EI and EF plants (Table 2). The presence of *Erwinia* sp. decreased the content of lauric acid (0.85-fold), maleic acid (0.60-fold), L-(-)-malic acid (0.62-fold), uridine 5'-diphosphogalactose (0.14-fold), D-glucose 6-phosphate (0.42-fold), 7-methylxanthine (0.53-fold), α,α-trehalose (0.18-fold), theophylline (0.34-fold)3-hydroxy-3-methylglutaric acid (0.44-fold) compared with EF. But increased the content of benzoic acid (4.14-fold), dulcitol (22.75-fold), azelaic acid (1.98-fold), gluconic acid (2.42-fold), guanosine (4.61-fold), thymidine (6.97-fold), L-(+)-lactic acid (17.69-fold), asparagine (10.31-fold), succinic acid (36.88-fold), citric acid (14.70-fold), 16-hydroxyhexadecanoic acid (17.89-fold), 2-oxobutyric acid (2.18-fold), pantothenic acid (3.62-fold), DL-β-leucine (8.36-fold), L-aspartic acid (9.08-fold), DL-tryptophan (17.62-fold), 2-furoic acid (6.52-fold), L-histidine (9.05-fold), 2-oxoglutaric acid (12.34-fold), hexadecanedioic acid (8.26-fold), trans-aconitic acid (12.92-fold), and sulfuric acid (2.21-fold). A total of 31 differentially expressed metabolites of EI and EF plants in ESI-, with significant differences observed in the heat map (Figure 2b). Importantly, there were 4 identical significant metabolites change between EI and EF in ESI+ compared to ESI- by Venn diagram analysis of different metabolites (Figure 3), including Asparagine, Guanosine, L-Aspartic acid, and L-Histidine.
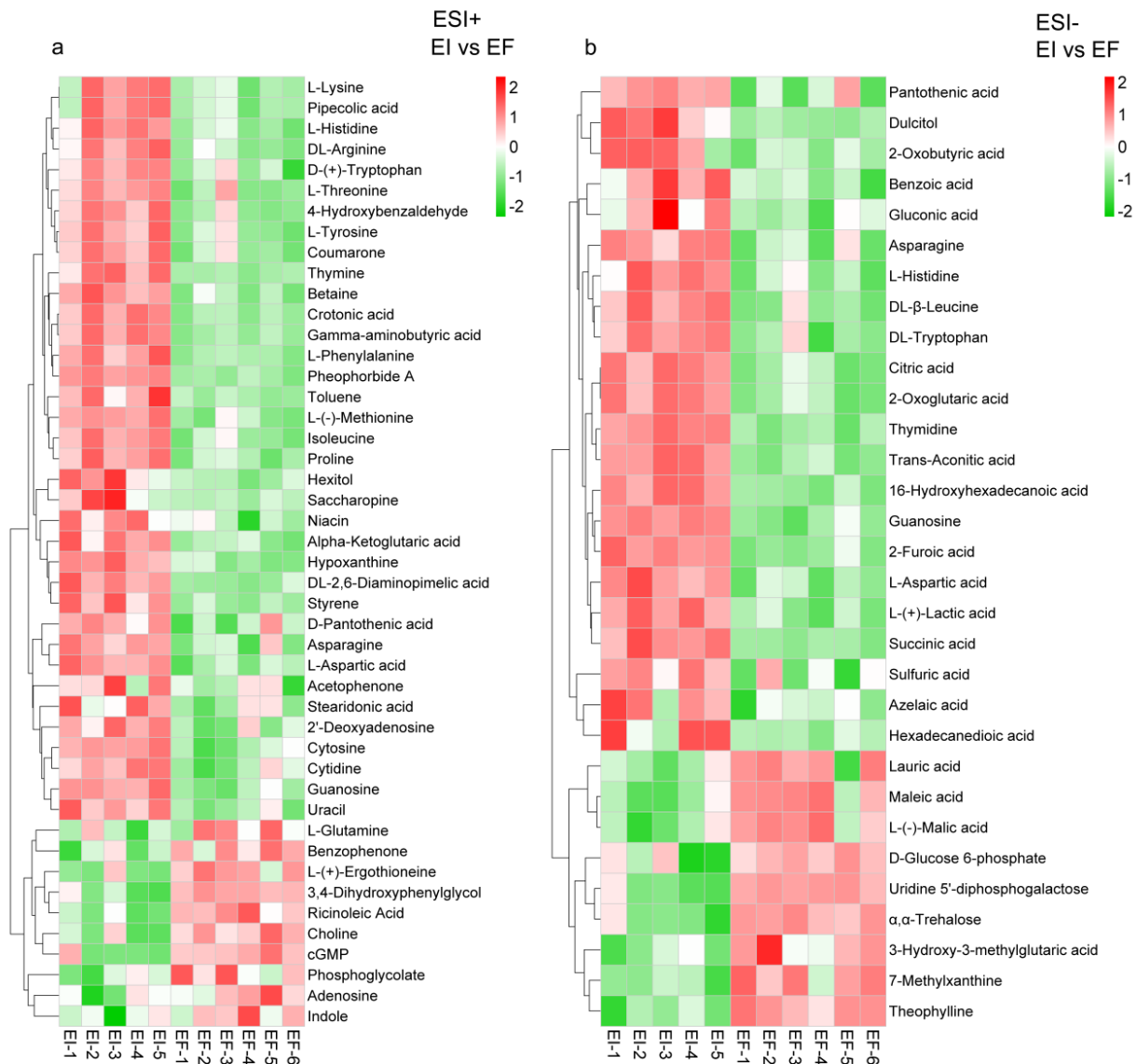

Figure 2 Hierarchical cluster analysis of the significantly different metabolites in stems of EI and EF plants under ESI+ and ESI-
Note: a shows 46 significantly different metabolites of EI and EF plants under ESI+; b shows 31 significantly different metabolites of EI and EF plants under ESI-

Table 2 Relative concentrations and fold changes of significantly different metabolites in EI and EF plants stem under ESI-

Metabolites name	EI	EF	$\text{Log}_2^{(EI/EF)}$
Lauric acid	2185.23±76.75	2561.40±133.56	-0.23 *
Benzoic acid	237.55±58.58	57.34±8.13	2.05 **
Dulcitol	2305.40±847.65	101.36±9.08	4.51 *
Azelaic acid	1356.31±217.86	685.21±79.05	0.99 *
Gluconic acid	3761.02±1026.32	1553.78±177.06	1.28 *
Guanosine	1064.40±48.94	230.99±39.95	2.20 ***
Thymidine	535.25±48.61	76.83±8.12	2.80 ***
Maleic acid	3491.83±332.91	5800.03±435.08	-0.73 **
L-(+)-Lactic acid	12354.45±3222.63	698.40±190.64	4.14 **
Asparagine	6529.11±1176.52	633.30±289.78	3.37 ***
L-(-)-Malic acid	114357.52±12545.86	184766.67±14416.32	-0.69 **
Succinic acid	17430.83±5313.10	472.63±42.99	5.20 **
Citric acid	12996.81±2243.72	883.90±252.64	3.88 ***
Uridine 5'-diphosphogalactose	240.22±127.86	1691.41±103.38	-2.82 ***
16-Hydroxyhexadecanoic acid	739.17±130.94	41.31±7.38	4.16 ***
2-Oxobutyric acid	87.14±13.47	39.94±3.16	1.13 **
Pantothenic acid	293.72±30.50	81.17±41.58	1.86 **
DL-β-Leucine	768.55±161.59	91.94±37.64	3.06 **
D-Glucose 6-phosphate	539.04±207.72	1296.25±114.49	-1.27 **
7-Methylxanthine	4963.71±348.58	9360.19±821.13	-0.92 **
L-Aspartic acid	3248.79±778.10	357.87±77.56	3.18 **
α,α-Trehalose	2987.32±1346.12	16466.27±1535.58	-2.46 ***
Theophylline	5104.69±745.54	15225.50±1229.79	-1.58 ***
DL-Tryptophan	2009.44±502.48	114.03±80.06	4.14 **
2-Furoic acid	710.85±69.46	109.01±21.48	2.71 ***
3-Hydroxy-3-methylglutaric acid	813.23±126.43	1862.65±320.93	-1.20 *
L-Histidine	773.47±191.49	85.45±27.35	3.18 **
2-Oxoglutaric acid	12217.96±1921.88	990.38±249.58	3.62 ***
Hexadecanedioic acid	166.86±57.66	20.31±2.46	3.04 *
Trans-aconitic acid	1853.20±291.94	143.44±26.69	3.69 ***
Sulfuric acid	8075.24±1046.23	3654.87±977.53	1.14 *

Note: Fold changes were calculated using the formula $\text{log}_2^{(EI/EF)}$. *, **; *** means significant differences at $0.01<p<0.05$; $0.001<p<0.01$ and $p<0.001$, respectively
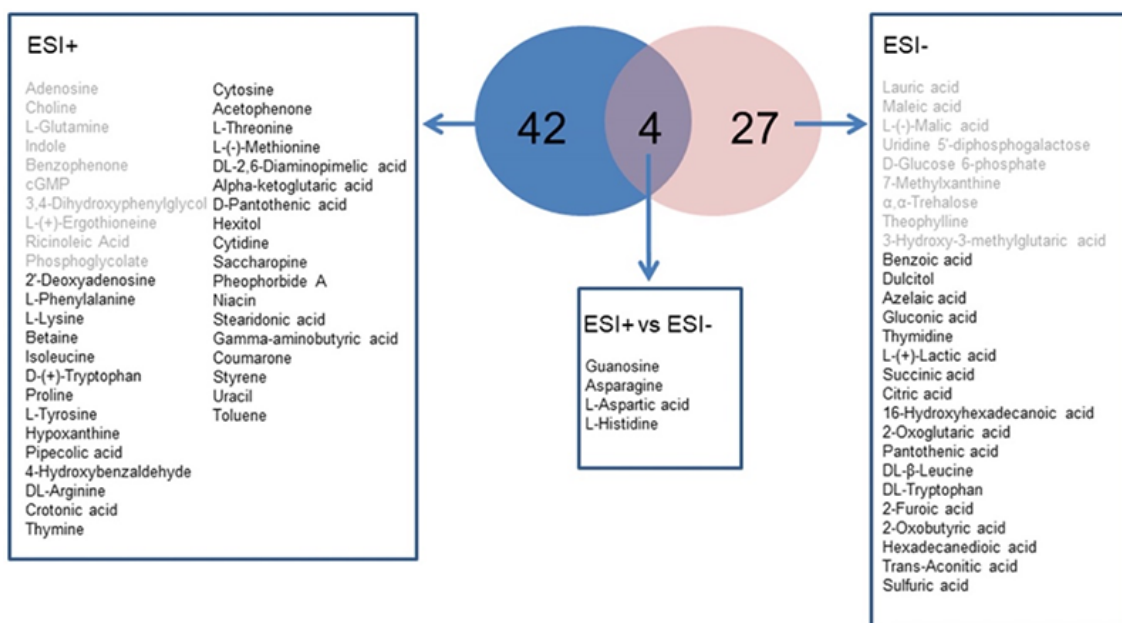

Figure 3 Venn diagram analysis of different metabolites between EI and EF plants under ESI+ and ESI-

Note: The overlapping regions of the Venn indicate the metabolites shared between corresponding groups in the experimental comparisons, and the remaining regions shows the specifically metabolites

1.3 Effects of *Erwinia* sp. on the metabolic pathways of *D. officinale* under ESI+ and ESI- conditions

To investigate the differences in metabolic pathways of EI and EF plants, impact values were estimated by pathway topology analysis and P values by the enrichment analysis. Using MetaboAnalyst 5.0 to analyze metabolic pathways, we found that alanine, aspartate and glutamate metabolism, phenylalanine metabolism, isoquinoline alkaloid biosynthesis, lysine degradation, and lysine biosynthesis might be the most relevant pathways for differential regulation by *Erwinia* sp. in *D. officinale* under ESI+ conditions (Figure 4a). Similarly, citrate cycle (TCA cycle), cutin, suberine, and wax biosynthesis, alanine, aspartate, and glutamate metabolism, pyruvate metabolism, starch, and sucrose metabolism, and glyoxylate and dicarboxylate metabolism might be the most relevant pathways responsible for differential expression after *Erwinia* sp. invasion of stem segments under ESI- conditions (Figure 4b). Thus, *Erwinia* sp. reprogrammed different physiological processes in the host plants and made the condition of *D. officinale* worse.
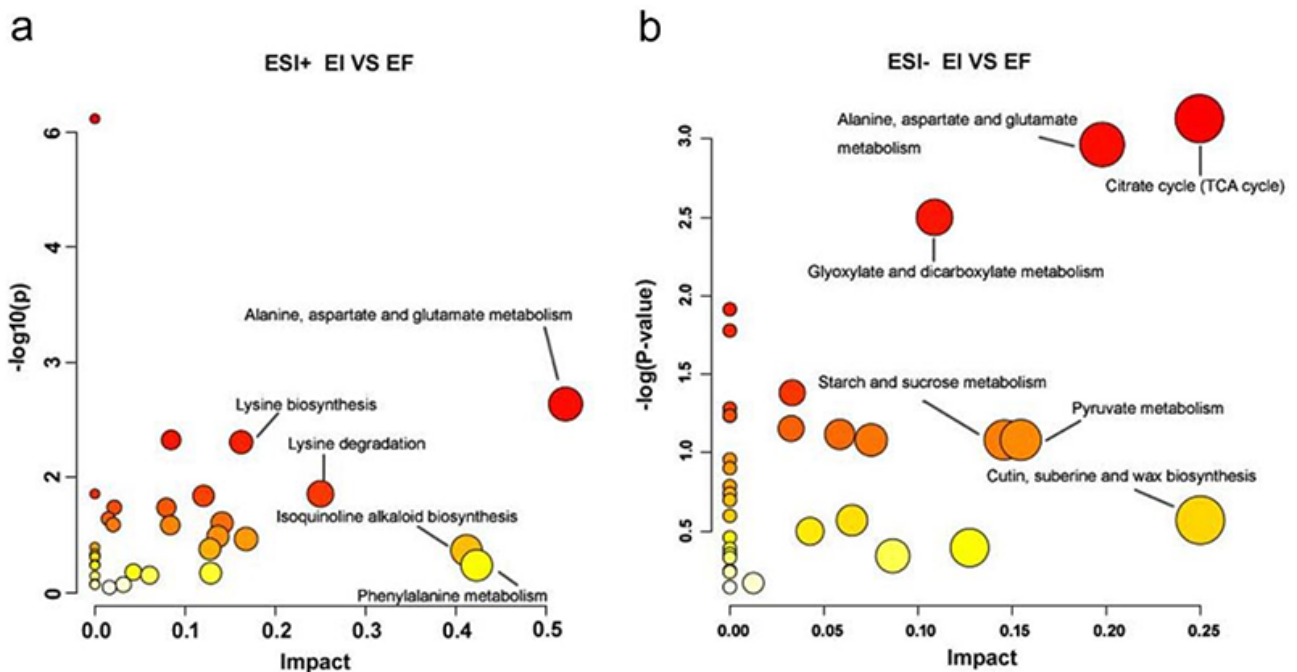

Figure 4 The pathway enrichment analysis

Note: a and b represent for the significantly changed pathway between EI and EF plants under ESI+ and ESI-, respectively (EI vs EF under ESI+, EI vs EF under ESI-)

2 Discussion

Dendrobium officinale has a long history of traditional Chinese herbal medicine in China. Previous studies mainly focused on the medicinal components (Cao et al., 2019), seed germination (Tan et al., 2014), and the methods of polysaccharide extraction (He et al., 2018; Liang et al., 2019). However, there are fewer studies on the metabolic changes of *D. officinale* happen after pathogenic infection. In our study, we used metabolomics techniques to analyze the metabolites of EI and EF plants. After infection, plant metabolism and morphology are greatly altered. Plants may inhibit pathogen growth by producing toxic substances, as well as altering metabolic processes by producing corresponding signaling molecules (Arbona and Gómez-Cadenas, 2015).

After pathogens invasion, the content of amino acids, nucleic acids, alkaloids, and saccharides gradually increase in plants (Parker et al., 2009; Jones et al., 2011). Suharti (2016) et al. demonstrated that parabens increases in *Rhizoctonia solani* infected rice plants which subsequently triggers programmed cell death in the plant due to pathogen infestation, as a self-defense mechanism of the plant. In addition, p-hydroxybenzoic acid can inhibit the growth of pathogenic bacteria. The increased content of 4-hydroxybenzaldehyde in our study was an effective response to *Erwinia* sp. disease following infestation. The C metabolism provides energy for N metabolism while N metabolism provides the necessary enzymes for C metabolism in plants (Zhang et al., 2017). *Dendrobium*

officinale infested with *Erwinia* sp. affected the TCA cycle as well as acetaldehyde and dicarboxylic acid metabolism by increasing the organic acid content of citric acid, cis-aconitate, α-ketoglutarate, and succinic acid in the body. Among them, citric acid was the key metabolite in glyoxylate and dicarboxylic acid metabolism and TCA cycle and was able to produce energy in response to adverse environmental disturbances (Chen et al., 2019).

In terms of changes in the content of amino acids in plants, the content of lysine, isoleucine, aspartic acid, asparagine, methionine, and proline was significantly increased in EI plants compared to EF plants. *Erwinia* sp. changed the pathways of alanine, aspartic acid, and glutamic acid metabolism, and phenylalanine metabolism in *D. officinale*. Proline is a reactive oxygen scavenger that activates various antioxidant enzymes related to the scavenging of reactive oxygen species, protects cells from damage caused by singlet oxygen and hydroxyl radicals, etc., and keeps proteins, DNA, and membrane structures in cells in a stable state (Li et al., 2018). Proline also provides additional compatible osmotic electrolytes to regulate osmotic pressure and to regulate intracellular pH (Miller et al., 2010). Lysine has a regulatory effect on plant photosynthesis, and the EI plant regulates its photosynthesis by altering lysine degradation and biosynthesis metabolism (Lin et al., 2008). The degradation of lysine can produce acetyl coenzyme A, which then enters the tricarboxylic acid cycle (TCA cycle). Moreover, the content of γ-aminobutyric acid, which protects plants from oxidative reactions by regulating lipid acidity, was increased in EI plants (Nikiforova et al., 2018).

During the metabolism of amino acids, secondary metabolites such as alkaloids and flavonoids are also synthesized (Sumner et al., 2003). The content of betaine was higher in EI than EF plants, which can protect intracellular proteins and metabolic enzymes and maintains enzyme activity as well as cell membrane stability (Goel et al., 2011). Flavonoids are a class of secondary metabolites widely distributed in plants, highly diversified in structure, and involved in many life processes in plants, which mainly play a role in defense against pathogens and protection against stress-induced injury (Arbona and Gómez-Cadenas, 2015). Flavonoids are different in content depending on the functions undertaken by plant organs. For example, when plant leaves are subjected to strong light or UV stress, the leaves synthesize large amounts of flavonoids, which facilitate the absorption of UV light and protect the plant from damage. And bark produces flavonoid phytochemicals to resist damage when it is damaged by microorganisms as well as phytophagous insects (Zhu et al., 2007). EI plants mainly by increasing the content of coumarones, which are precursors of flavonoids and can be transformed by plant metabolism to produce flavonoids and inhibit the enzymes secreted by pathogenic bacteria to degrade the cell wall, thereby protecting the integrity of the plant cell wall (Chai et al., 2017).

It has been shown that sugar can act as an osmotic protectant like amino acids to protect plants under extreme salt, drought, and desiccation stresses (Shulaev et al., 2008). Saccharide not only regulates the osmotic pressure of plant cells but is also a component of plant cell membranes and cell walls (O'Donoghue et al., 2009). *Erwinia* sp. increases the content of sugars (hexitol, dulcitol) and fatty acids (Stearidonic acid, 16-hydroxyhexadecanoic acid) in the plant to alter the metabolic pathways of cutin, suberine, and wax biosynthesis. Cutin is an important component of the cuticle and plays a vital role in the plant's response to pathogen infection that protects the plant and is also a medium for the exchange of water, gases, and nutrients (Li et al., 2019). In addition, Mahatma (2019) et al. showed that peanuts infested with *Alternaria alternate* showed increased levels of taxonomic substances, with the phenolics binding to the fungal cell wall and thus making it impermeable to water, thus blocking further growth and the uptake of water and other nutrients by the fungus. Similarly, the amount of coumarone in the *D. officinale* increases to protect the plant against the disease when *Erwinia* sp. infests the plant.

It is worth mentioning that the content of trehalose and glucose 6-phosphate in EI plants in this study was reduced compared to EF plants. Among them, trehalose is the most effective protector of cell membranes, cytoplasm, and proteins. *Erwinia* sp. mainly reduces the content of α,α-trehalose to reduce the stability of plant cell membranes (Zhao et al., 2020). In addition, glucose 6-phosphate can produce NADH catalyzed by glucose 6-phosphate dehydrogenase, which is used to protect the oxidative balance in plants (Yang et al., 2019). The changes of α,α-trehalose, and glucose 6-phosphate affect the starch and sucrose metabolic pathways. Usually, the α,α-trehalose as well as glucose 6-phosphate content in the body is increased when plants are subjected to

pathogens. However, since α,α-trehalose, and glucose 6-phosphate are intermediate products in the metabolic process, it is possible that α,α-trehalose is further hydrolyzed to produce glucose during the metabolic process, which is then oxidized to produce gluconic acid. And glucose 6-phosphate may be broken down through the glycolytic pathway and then enter the TCA cycle process to produce substances such as citric acid. As the samples were collected from one growth time point of *D. officinale*, there was no continuity for the detection of metabolites, so the α,α-trehalose, and glucose-6 phosphate content of the assay was down-regulated. However, most of the indicative metabolite contents increased in the experiment, therefore, our study suggests that the metabolic pathway was reorganized after *Erwinia* sp. infecting the *D. officinale*. Plants improve their disease resistance by consuming the original plant sugars to provide energy to feed other metabolic pathways and by producing the corresponding antimicrobial substances.

3 Materials and Methods

3.1 *D. officinale* plants and preparation of LC-MS

Dendrobium officinale were collected from Xicheng Xiushu Agriculture and Forestry base, Anlong County, Qianxinan Prefecture, Guizhou Province in 2019 (105°42′E, 24°99′N). Five EI and six EF plants were randomly selected, carefully transferred to 5 mL centrifuge tubes, and immediately placed in -80°C liquid nitrogen for freezing. A 50 mg of freeze-dried sample was taken in a 5 mL EP tube and extracted with 800 μL of 80% methanol, then vortexed and mixed for 30 s. The mixture was ground to fine powder using Grinding Mill at 60 Hz for 90 s, ultrasonicated for 30 min at 4°C, vortexed and mixed for 3°C. The samples were re-vortexed for 30 s and kept for 30 min at 4°C. Next, they were centrifuged at 12,000 rpm and 4°C for 15 min, all supernatant was transferred to another 1.5 mL EP tube, kept at -40°C for 1 h, and again centrifuged at 12,000 rpm for 15 min. Finally, 200 μL of supernatant was added to 5 μL of internal standard (700 μg/mL, DL-o-Chlorophenylalanine), then transferred to a vial for LC-MS analysis.

3.2 LC-MS analysis

Analysis was performed using LC-MS (Thermo, Ultimate 3000LC, Orbitrap Elite), which was based on a Waters ACQUITY UPLC HSS T3 column (2.1 mm × 100 mm, 1.8 μm). The mobile phase A (95% water + 5% acetonitrile + 0.1% formic acid) and eluent B (98% acetonitrile + 2% water + 0.1% formic acid) with a flow rate of 0.3 mL/min, a column temperature of 40°C, an Automatic injector temperature of 4°C, and an injection volume of 4 μL were employed. The positive and negative ion detection modes of the electrospray ionization source were used (Xu et al., 2020), and the conditions of the electrospray ionization source were set as follows: Electrospray ionization in positive ion mode (ESI+): heater temperature 300°C; sheath gas flow rate: 45 arb; auxiliary gas flow rate: 15 arb; tail gas flow rate: 1 arb; electrospray voltage: 3.0 KV; capillary temperature: 350°C; S-Lens RF Level, 30%. Electrospray ionization in negative ion mode (ESI-): heater temperature 300°C; sheath gas flow rate: 45 arb; auxiliary gas flow rate: 15 arb; exhaust gas flow rate: 1 arb; electrospray voltage: 3.2 KV; capillary temperature: 350°C; S-Lens RF Level, 60%.

3.3 Statistical analysis

Our experiment was performed using SIMCA-P 14.0 software for multivariate statistical analysis, including PCA (Unsupervised principal components analysis) and OPLS-DA (Orthogonal Partial Least Squares-Discriminant Analysis), and the data were also analyzed with independent t-tests, with $p<0.05$ being considered a statistically significant difference. The VIP is a weighted sum of the OPLS-DA squares (Jia et al., 2019). In addition, differential metabolites were identified by independent samples t-test ($p<0.05$) and VIP (VIP>1). Subsequently, the metabolites were identified by MetaboAnalyst (http://MetaboAnalyst.ca/) for different metabolites to identify metabolic pathways.

Reference

Arbona V., and Gómez-Cadenas A., 2015, Metabolomics of disease resistance in crops, Current Issues in Molecular Biology, 19(1): 13-30

Balamurugan A., Kumar A., Sakthivel K., Ashajyothi M., Sahu K.P., and Karthikeyan M., 2020, Characterization of *Dickeya* fangzhongdai causing bacterial soft rot disease on *Dendrobium nobile* in India, European Journal of Plant Pathology, 158(3): 773-780
https://doi.org/10.1007/s10658-020-02094-7

Chai R.J., and Lei J.S., 2017, Effects of Ce(NO$_3$)3 and p-coumaric acid on synthesis of flavonoids from *Aspergillus Niger*, Journal of the Chinese Society of Rare Earths, 6: 117-123

Cao H., Ji Y., Li S., Lu L., Tian M., Yang W., and Li H., 2019, Extensive metabolic profiles of leaves and stems from the medicinal plant *Dendrobium officinale* Kimura et Migo, Metabolites, 9(10): 215
https://doi.org/10.3390/metabo9100215
PMid:31590300 PMCid:PMC6835975

Chen C., Liu H., Wang C., Liu Z., Liu X., Zou L., Zhao H., Yan Y., Shi J., and Chen S., 2019, Metabolomics characterizes metabolic changes of *Apocyni Veneti Folium* in response to salt stress, Plant Physiol Biochem, 144: 187-196
https://doi.org/10.1016/j.plaphy.2019.09.043
PMid:31585397

Feng J., 2017, Recent advances in taxonomy of plant pathogenic bacteria, Scientia Agricultura Sinica, 50(12): 2305-2314

Goel D., Singh A.K., Yadav V., Babbar S.B., Murata N., and Bansal K.C., 2011, Transformation of tomota with a bacterial coda gene enhances tolerance to salt and water stresses, Journal of Plant Physiology, 168(11): 1286-1294
https://doi.org/10.1016/j.jplph.2011.01.010
PMid:21342716

He L., Yan X., Liang J., Li S., He H., Xiong Q., Lai X., Hou S., and Huang S., 2018, Comparison of different extraction methods for polysaccharides from *Dendrobium officinale* stem, Carbohydr Polym, 198: 101-108
https://doi.org/10.1016/j.carbpol.2018.06.073
PMid:30092979

Hua G.K.H., Ali E., and Ji P., 2019, Characterization of bacterial pathogens causing fruit soft rot and stem blight of bell pepper in Georgia, USA, Journal of Plant Pathology, 102(2): 311-318

Jia G., Sha K., Feng X., and Liu H., 2019, Post-thawing metabolite profile and amino acid oxidation of thawed pork tenderloin by HVEF-A short communication, Food Chem, 291: 16-21
https://doi.org/10.1016/j.foodchem.2019.03.154
PMid:31006455

Jones O.A.H., Maguire M.L., Griffin J.L., Jung Y.H., Shibato J., Rakwal R., Agrawal G.K., and Jwa N.S., 2011, Using metabolic profiling to assess plant-pathogen interactions: an example using rice (*Oryza sativa*) and the blast pathogen *Magnaporthe grisea*, European Journal of Plant Pathology, 129(4): 539-554
https://doi.org/10.1007/s10658-010-9718-6

Li M.X., Xu J.S., Wang X.X., Fu H., Zhao M.L., Wang H., and Shi L.X., 2018, Photosynthetic characteristics and metabolic analyses of two soybean genotypes revealed adaptive strategies to low-nitrogen stress, Journal of plant, 229: 132-141
https://doi.org/10.1016/j.jplph.2018.07.009
PMid:30081252

Li T., Wu Q., Zhu H., Zhou Y., Jiang Y., Gao H., and Yun Z., 2019, Comparative transcriptomic and metabolic analysis reveals the effect of melatonin on delaying anthracnose incidence upon postharvest banana fruit peel, BMC Plant Biol, 19(1): 289
https://doi.org/10.1186/s12870-019-1855-2
PMid:31262259 PMCid:PMC6604187

Liang J., Zeng Y., Wang H., and Lou W., 2019, Extraction, purification and antioxidant activity of novel polysaccharides from *Dendrobium officinale* by deep eutectic solvents, Nat Prod Res, 33(22): 3248-3253
https://doi.org/10.1080/14786419.2018.1471480
PMid:29726707

Lin B.G., Yang L.Y., Xiao L., and Zeng J., 2008, Mechanism of the inhibition effect of lysine on *Microcystis aeruginosa*, Journal of Agro-Environment Science, 27(4): 1561-1565

Nikiforova V.J., Kopka J., Tolstikov V., Fiehn O., Hopkins L., Hawkesford M.J., Hesse H., and Hoefgen R., 2018, Systems rebalancing of metabolism in response to sulfur deprivation, as revealed by metabolome analysis of *Arabidopsis* plants, Plant Physiol, 138(1): 304-318
https://doi.org/10.1104/pp.104.053793
PMid:15834012 PMCid:PMC1104185

Mahatma M.K., Thawait L.K., Jadon K.S., Rathod K.J., and Golakiya B.A., 2019, Distinguish metabolic profiles and defense enzymes in *Alternaria* leaf blight resistant and susceptible genotypes of groundnut, Physiology and Molecular Biology of Plants, 25(6): 1395-1405
https://doi.org/10.1007/s12298-019-00708-x
PMid:31736543 PMCid:PMC6825051

Mayo-Prieto S., Marra R., Vinale F., Rodriguez-Gonzalez A., Woo S.L., Lorito M., Gutierrez S., and Casquero P.A., 2019, Effect of trichoderma velutinum and *Rhizoctonia solani* on the metabolome of bean plants (*Phaseolus vulgaris* L.), International Journal Molecular Sciences, 20(3): 549
https://doi.org/10.3390/ijms20030549
PMid:30696057 PMCid:PMC6387467

Miller G., Suzuki N., Ciftci-Yilmaz S., and Mittler R., 2010, Reactive oxygen species homeostasis and signalling during drought and salinity stresses, Plant Cell Environ, 33(4): 453-467
https://doi.org/10.1111/j.1365-3040.2009.02041.x
PMid:19712065

Obata T., and Fernie A.R., 2012, The use of metabolomics to dissect plant responses to abiotic stresses, Cell Mol Life Sci, 69(9): 3225-3243
https://doi.org/10.1007/s00018-012-1091-5
PMid:22885821 PMCid:PMC3437017

O'Donoghue E.M., Somerfield S.D., Watson L.M., Brummell D.A., and Hunter D.A., 2009, Galactose metabolism in cell walls of opening and senescing petunia petals, Planta, 229(3): 709-721
https://doi.org/10.1007/s00425-008-0862-6
PMid:19082620

Parker D., Beckmann M., Zubair H., Enot D.P., Caracuel-Rios Z., Overy D.P., Snowdon S., Talbot N.J., and Draper J., 2009, Metabolomic analysis reveals a common pattern of metabolic reprogramming during invasion of three host plant species by *Magnaporthe grisea*, Plant J, 59(5): 723-737
https://doi.org/10.1111/j.1365-313X.2009.03912.x
PMid:19453445

Pavlík M., Pavlíková D., and Vašíčková S., 2010, Infrared spectroscopy-based metabolomic analysis of maize growing under different nitrogen nutrition, Plant Soil & Environment, 56(11): 533-540

Qiu D.S., Liu X.J., Zhen J.R., Cai S.K., Zhen X.L., Luo H.M., and Li W., 2011, The main diseases of *Dendrobium officinale* and their control in greenhouse, Guangdong Agricultural Science, S1: 126-128

Razzaq A., Sadia B., Raza A., Khalid H.M., and Saleem F., 2019, Metabolomics: A way forward for crop improvement, Metabolites, 9(12): 303
https://doi.org/10.3390/metabo9120303
PMid:31847393 PMCid:PMC6969922

Sade D., Shriki O., Cuadros-Inostroza A., Tohge T., Semel Y., Haviv Y., Willmitzer L., Fernie A.R., Czosnek H., and Brotman Y., 2014, Comparative metabolomics and transcriptomics of plant response to *Tomato yellow leaf curl virus* infection in resistant and susceptible tomato cultivars, Metabolomics, 11(1): 81-97
https://doi.org/10.1007/s11306-014-0670-x

Shulaev V., Cortes D., Miller G., Mittler R., 2008, Metabolomics for plant stress response, Physiol Plant, 132(2): 199-208
https://doi.org/10.1111/j.1399-3054.2007.01025.x
PMid:18251861

Suharti W.S., Nose A., and Zheng S.H., 2016, Metabolomic study of two rice lines infected by *Rhizoctonia solani* in negative ion mode by CE/TOF-MS, Journal of Plant Physiology, 206: 13-24
https://doi.org/10.1016/j.jplph.2016.09.004
PMid:27688090

Sung J., Lee S., Lee Y., Ha S., Song B., Kim T., Waters B.M., and Krishnan H.B., 2015, Metabolomic profiling from leaves and roots of tomato (*Solanum lycopersicum* L.) plants grown under nitrogen, phosphorus or potassium-deficient condition, Plant Sci, 241: 55-64
https://doi.org/10.1016/j.plantsci.2015.09.027
PMid:26706058

Sumner L.W., Mendes P., Dixon R.A., 2003, Plant metabolomics: large-scale phytochemistry in the functional genomics era, Phytochemistry, 62(6): 817-836
https://doi.org/10.1016/S0031-9422(02)00708-2

Tan X.M., Wang C.L., Chen X.M., Zhou Y.Q., Wang Y.Q., Luo A.X., Liu Z.H., and Guo S.X., 2014, In vitro seed germination and seedling growth of an endangered epiphytic orchid, *Dendrobium officinale*, endemic to China using mycorrhizal fungi (*Tulasnella* sp.), Scientia Horticulturae, 165: 62-68
https://doi.org/10.1016/j.scienta.2013.10.031

Wang D.K., Ji X.T., Zhan H.X., Zheng C.P., Wang W.M., Wu J.J., Zong H., Wang F.L., Tan X.L., and Wang X.Q., 2021, Comparative study on the efficacies of 11 chemical agents against taro soft rot caused by *Pectobacterium aroidearum*, Plant Diseases and Pests, 12(2): 4

Wang H., Fang H., Wang Y., Duan L., and Guo S., 2011, In situ seed baiting techniques in *Dendrobium officinale* Kimuraet Migo and *Dendrobium* nobile Lindl. : the endangered Chinese endemic Dendrobium (Orchidaceae), World Journal of Microbiology and Biotechnology, 27(9): 2051-2059
https://doi.org/10.1007/s11274-011-0667-9

Xu Z., Li L., Xu Y., Wang S., Zhang X., Tang T., Yu J., Zhao H., Wu S., Zhang C., and Zhao X., 2020, Pesticide multi-residues in *Dendrobium officinale* Kimura et Migo: Method validation, residue levels and dietary exposure risk assessment, Food Chem, 343: 128490
https://doi.org/10.1016/j.foodchem.2020.128490
PMid:33158673

Yang L., Wang X., Chang N., Nan W., Wang S., Ruan M., Sun L., Li S., and Bi Y., 2019, Cytosolic glucose-6-phosphate dehydrogenase is involved in seed germination and root growth under salinity in *Arabidopsis*, Front Plant Sci, 10: 182
https://doi.org/10.3389/fpls.2019.00182
PMid:30873191 PMCid:PMC6401624

Yuan Y., Tang X., Jia Z., Li C., Ma J., and Zhang J., 2020, The Effects of ecological factors on the main medicinal components of *Dendrobium officinale* under different cultivation modes, Forests, 11(1): 94
https://doi.org/10.3390/f11010094

Zhang X., Li K., Xing R., Liu S., and Li P., 2017, Metabolite profiling of wheat seedlings induced by *Chitosan*: revelation of the enhanced carbon and nitrogen metabolism, Front Plant Sci, 8: 2017
https://doi.org/10.3389/fpls.2017.02017
PMid:29234335 PMCid:PMC5712320

Zhao M., Guo R., Li M., Liu Y., Wang X., Fu H., Wang S., Liu X., and Shi L., 2020, Physiological characteristics and metabolomics reveal the tolerance mechanism to low nitrogen in Glycine soja leaves, Physiol Plant, 168(4): 819-834
https://doi.org/10.1111/ppl.13022
PMid:31593297

Zhu H., Hu H.Y., Lu C.Y., and Li X., 2007, Progresses on flavonoid metabolism in plants and it's regulation, Journal of Xiamen University (Natural Science), S1: 136-143

Zimnoch-Guzowska E., Lebecka R., and Pietrak J., 1999, Soft rot and blackleg reactions in diploid potato hybrids inoculated with *Erwinia* spp, American Journal of Potato Research, 76(4): 199-207
https://doi.org/10.1007/BF02854222

Zuo S.M., Yu H.D., Zhang W., Zhong Q., Chen W., Chen W., Yun Y.H., and Chen H., 2020, Comparative metabolomic analysis of *Dendrobium officinale* under different cultivation substrates, Metabolites, 10(8): 325
https://doi.org/10.3390/metabo10080325
PMid:32785071 PMCid:PMC7465462